Volume 17 | Number 45 | 7 December 2015 | Pages 8565–8764

CrystEngComm

www.rsc.org/crystengcomm

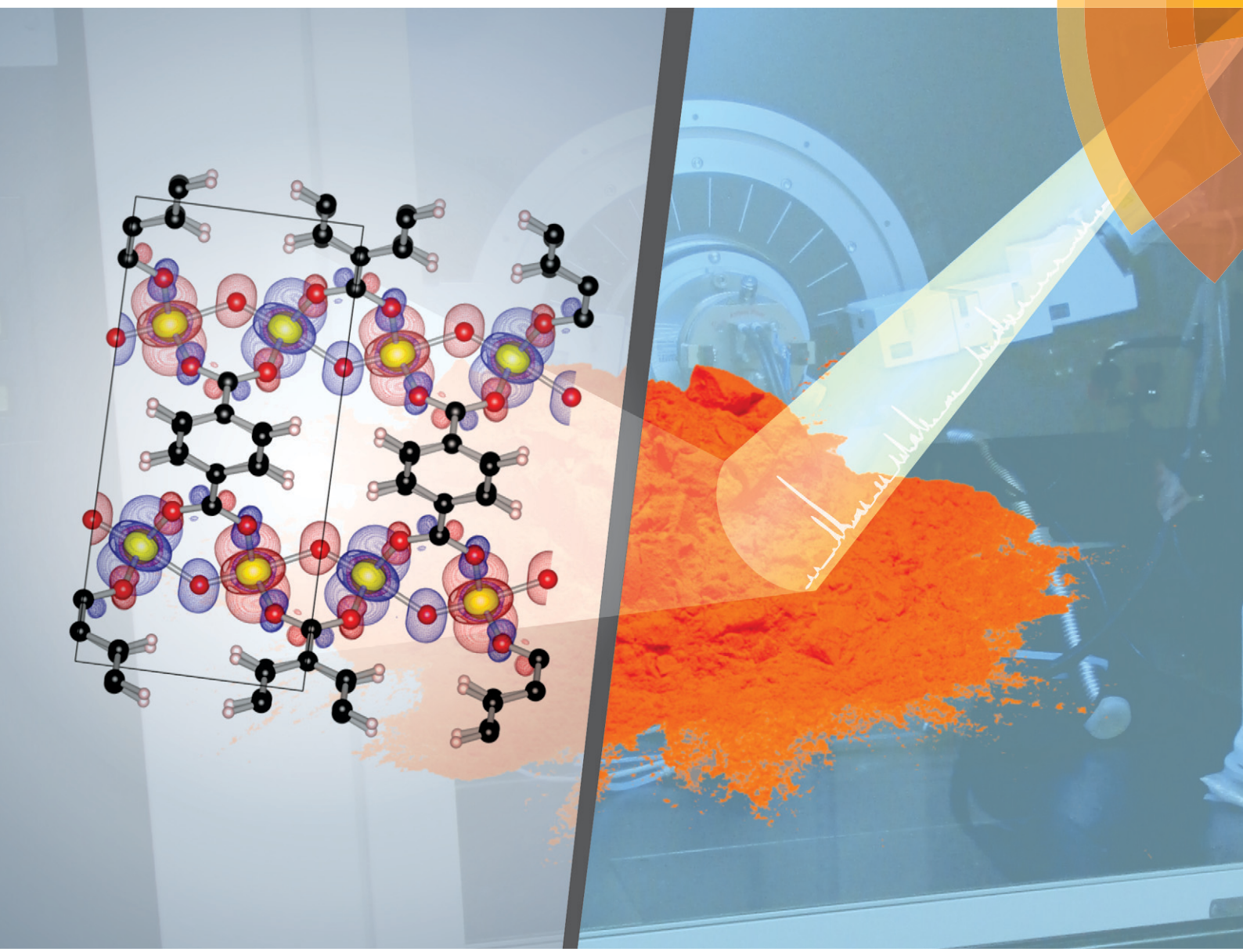

ROYAL SOCIETY OF CHEMISTRY

PAPER

Pascal Van Der Voort, Veronique Van Speybroeck *et al.*

Fine-tuning the theoretically predicted structure of MIL-47(V) with the aid of powder X-ray diffraction

CrystEngComm

PAPER

Cite this: *CrystEngComm*, 2015, **17**, 8612

Fine-tuning the theoretically predicted structure of MIL-47(V) with the aid of powder X-ray diffraction†

Thomas Bogaerts,[ab] Louis Vanduyfhuys,[a] Danny E. P. Vanpoucke,[ab] Jelle Wieme,[a] Michel Waroquier,[a] Pascal Van Der Voort*[b] and Veronique Van Speybroeck*[a]

Received 15th July 2015,
Accepted 8th September 2015

DOI: 10.1039/c5ce01388g

www.rsc.org/crystengcomm

The structural characterization of complex crystalline materials such as metal organic frameworks can prove a very difficult challenge both for experimentalists as for theoreticians. From theory, the flat potential energy surface of these highly flexible structures often leads to different geometries that are energetically very close to each other. In this work a distinction between various computationally determined structures is made by comparing experimental and theoretically derived X-ray diffractograms which are produced from the materials geometry. The presented approach allows to choose the most appropriate geometry of a MIL-47(V) MOF and even distinguish between different electronic configurations that induce small structural changes. Moreover the techniques presented here are used to verify the applicability of a newly developed force field for this material. The discussed methodology is of significant importance for modelling studies where accurate geometries are crucial, such as mechanical properties and adsorption of guest molecules.

Introduction

Computational modelling is often used to assist in the structure determination from powder diffraction patterns. Very elusive structures such as the geometry of γ-alumina could be resolved by proposing the detailed geometry from computations and using this in further refinements.[1] In the research on covalent organic frameworks, the use of initial geometries generated from molecular mechanics calculations has become indispensable for structure refinement.[2,3] This is mostly due to the fact that these materials cannot be synthesized as single crystals and structure determination has to be done with powder patterns, which is more prone to ambiguity. In the research on metal–organic frameworks (MOFs) this approach has also proven its merits, for example the well-known MIL-101 structure could only be refined with a structured database search combining metal nodes and linkers in different topologies.[4] Other MOF structures could be resolved *via* initial guesses of the structure provided by DFT simulations.[5] Again these techniques have to be applied since the materials are hard to obtain as single crystals.

Flexible MOFs are characterized by very flat potential energy surfaces, making *ab initio* structure optimization and structure determination a highly non-trivial exercise.[6–8] Variations in the atomic structure, often have a very strong influence on the calculated stability, electronic structure and physical properties. For example, in their construction of the CoRE database, Chung *et al.*[9] investigated the methane adsorption in MIL-53(Al) for the different published, experimental MIL-53(Al) geometries. They found that the methane uptake varied about 48% in the set of structures, while the void fractions only varied about 10%. The authors discussed the influence that proximal framework atoms have in the presence of adsorption sites and concluded that the exact atomic structure plays a very important role. The same observation was made by Lawler *et al.*[10] who showed the importance of an accurate crystal structure for gas sorption simulations.

In the computational research on metal organic frameworks the use of molecular mechanics methods has proven to be crucial for certain applications. For example, modelling diffusion phenomena or other physical effects that occur on longer length- or timescales cannot be done with quantum mechanical models. Due to the complexity of these materials, various force fields have been developed, each with their own strong features.[11–15] For the development of these molecular mechanics methods a comparison between the obtained

[a] *Center for Molecular Modelling (CMM), Ghent university, Technologiepark 903, 9052 Zwijnaarde, Belgium. E-mail: Veronique.vanspeybroeck@ugent.be*
[b] *Center for Ordered Materials, Organometallics and Catalysis (COMOC), Department of Inorganic and Physical Chemistry, Ghent University, Krijgslaan 281-S3, 9000 Ghent, Belgium. E-mail: pascal.vandervoort@ugent.be*
† Electronic supplementary information (ESI) available. See DOI: 10.1039/c5ce01388g

structures and experimental data on the crystal structure is very valuable to assess the ability of the force field to generate reliable geometries.

In this paper, computational models are not used for experimental structure validation, but a reverse procedure is adopted. We propose a methodology where results from an experimental powder XRD are used to aid in selecting between various *ab initio* models of MOF structures and to validate the structure obtained from a newly developed force field for MIL-47(V). In many cases theoretical calculations start from a model refined from a powder diffractogram. This is already a generally accepted practice in the modelling of crystalline materials such as zeolites[16–18] or MOFs[19,20] or other complex structures.[21] Currently it is not general practice to asses XRD patterns obtained from calculated geometries to experimental diffractograms. In this paper such a procedure is followed and applied to the well-known MIL-47(V) structure.

After the discovery of the MIL-47(V) structure, the Férey-group found a large pore structure belonging to the *Pnma* space group which contained displaced vanadium chains based on single crystal diffraction.[22] A slightly different structure with the *Pnma* space group, which didn't contain this displacement, was proposed by the Maurin-group as a result from molecular dynamics simulations.[23] Furthermore, in a previous work, Vanpoucke *et al.* showed that the spin configuration of the MIL-47(V) system is strongly correlated with its mechanical properties and stability, indicating the importance of having an accurate representation of the electronic structure.[6] Discrimination between the various structures is very challenging. The direct experimental measurement of the spin configuration is in practice almost impossible. Moreover, different authors have proposed structures for this MOF with small geometrical differences.[22,23] The current paper aims to unite well-defined X-ray diffractograms to resolve which modeled structure would be the most plausible. To that end, theoretical structures are determined from very accurate periodic structure calculations and also from a force field method derived from *ab initio* determined data. For the latter we have used a procedure proposed by some of the authors to quickly generate force fields for MOFs.[14] With the latter example we aim to verify how well the proposed force field can reproduce the *ab initio* calculations and how good it fits the experimental results.

Experimental details and computational methods

Experimental details

All chemicals were purchased from Sigma Aldrich and used without further purification. X-ray powder diffraction (XRPD) patterns were collected on a ARL X'TRA X-ray diffractometer with Cu Kα radiation of 0.15418 nm wavelength and a solid state detector, measurements were done over 48 h to improve the resolution. Nitrogen adsorption experiments were carried out at −196 °C using a Belsorp-mini II gas analyzer.

MIL-47 was synthesized as reported by Férey *et al.*[22] 1.37 g VCl3 and 0.36 g terephthalic acid were mixed in 15.7 mL of deionized H_2O. The resulting mixture was transferred in a Teflon-lined autoclave and kept a 200 °C for four days. After filtration the solid was washed with acetone and calcined at 300 °C for 24 h to obtain the final product. The Langmuir surface area was found to be 1150 $m^2\ g^{-1}$.

Computational details

Diffractograms were simulated from cif files with the aid of the mercury program.[24] Rietveld analysis and profile-only fitting was done with Jana2006.[25]

The *ab initio* structures used in this work are obtained from periodic Density Functional Theory (DFT) calculations, using the projector augmented wave (PAW) method and the generalized gradient approximation functional, as constructed by Perdew, Burke and Ernzerhof (PBE). Dispersion interactions are included through the damped DFT-D3 correction scheme.[26,27] Calculations were performed with the Vienna *ab initio* Simulation package (VASP).[28–32] The *ab initio* structures used are deposited with the Cambridge Crystallographic Data Center under the CCDC numbers: 1021380 (A^{FM}), 1021384 (A^{AF}), 1402266 (B^{FM}), 1402265 (B^{AF}). An overview of the computational methods is shown in Fig. 4.

The calculated geometries were obtained using a Monkhorst–Pack special *k*-point grid of 2 × 2 × 6 and the kinetic energy cutoff for the plane waves was set to 500 eV. Since the geometry of MIL-47(V) tends to collapse due to Pulay stresses,[33] the volume of the structures was optimized by fitting E(V) data to the Rose–Vinet equation of state.[34] This E(V) data was obtained through constant volume optimization of the structure at volumes in a range of ±4% around the equilibrium volume. With this constant volume, simultaneous optimizations of atomic positions and cell shape were done. The electronic configuration (ferromagnetic or anti-ferromagnetic) was imposed before each optimization, and verified afterward. Using the equilibrium volume obtained from the equation of state fit, a final geometry optimization was performed, optimizing both atomic positions and cell shape. With this approach, four different structures for MIL-47(V) were isolated by varying two aspects of the structure. Firstly, the spin configuration: we consider either ferromagnetic (FM) or anti-ferromagnetic (AF) V–O–V-chains (shown in Fig. 2). In previous work, it was shown that the chains are nearly non-interacting, with the latter spin-configuration representing the ground state spin structure, being about 280 meV more stable than the FM structure.[6] Secondly, there is the relative positioning of the vanadium chains. Here the displaced chain structure is 50 meV more stable than the non-displaced structure. This displacement of the second chain is indicated in Fig. 1. The resulting nomenclature used in this work is shown in Table 1. All the theoretical structures are compared with the published geometry of Férey *et al.*[22] that is deduced from single crystal measurements and with a newly measured PXRD pattern.

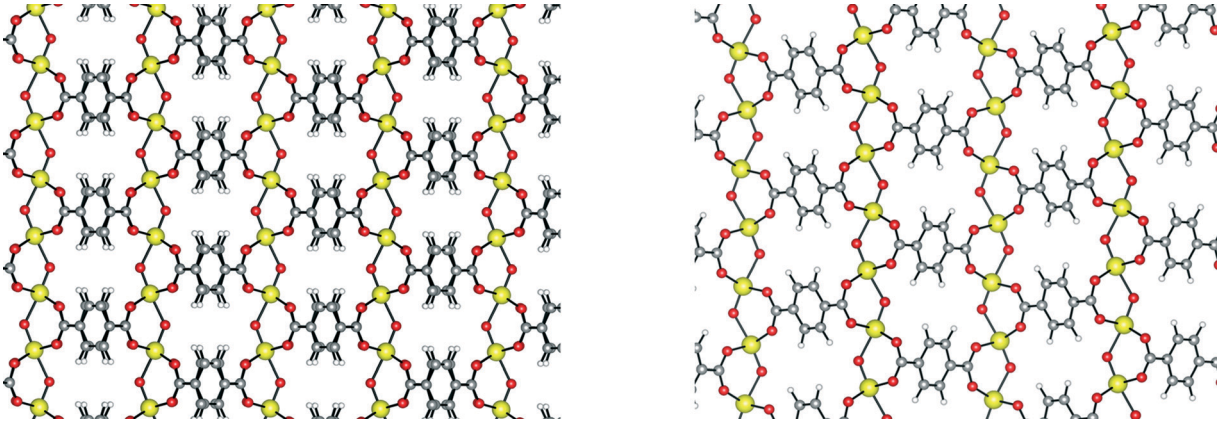

Fig. 1 Projection of the geometry without (left) and with (right) displaced vanadium chains.

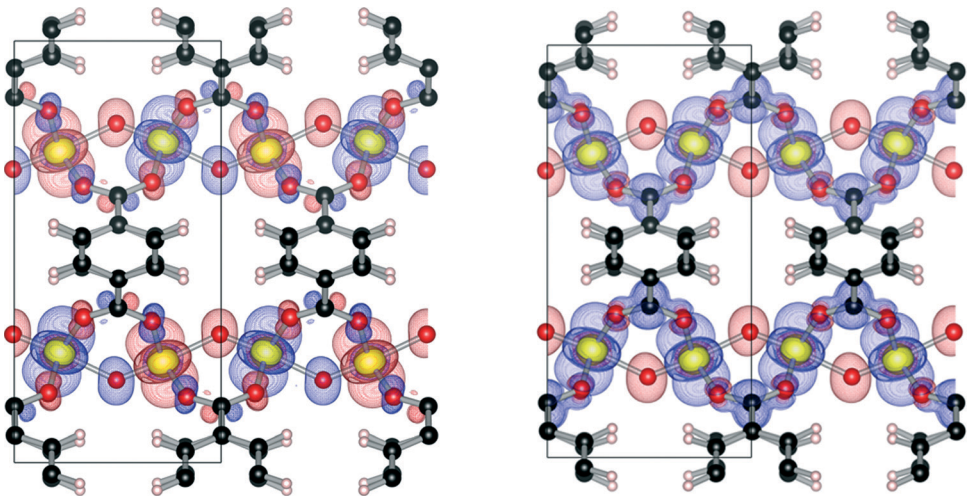

Fig. 2 Visualization of the spin densities for the anti-ferromagnetic (left) and the ferromagnetic (right) structure. Red orbitals are spin up, blue spin down.

To derive a fully flexible force field, QuickFF[14] used the isolated clusters shown in Fig. 3 as a training set. QuickFF is a software package to quickly derive force fields from *ab initio* training data. It was specifically designed for the derivation of force fields for metal–organic frameworks, but it can in principle be applied to a broader spectrum of materials including non-periodic molecular system. The required *ab initio* input data was generated using Gaussian09[35] by performing a geometry optimization followed by a frequency job to obtain the Hessian in equilibrium. Density Functional Theory was used with the B3LYP[36–38] functional and a 6-311G(d,p)[39,40] basis set. The covalent contributions to the force field were estimated using the QuickFF procedure. However, some *ad hoc* adaptations were implemented in order to better describe the asymmetry of the inorganic

Table 1 Energy differences of the different *ab initio* structures (meV per unit cell, (kJ per mol Vanadium))

	Spin configuration			
	Ferromagnetic		Anti-ferromagnetic	
Not displaced	A^{FM}	0 (0)	A^{AF}	−278 (−6.7)
Displaced	B^{FM}	−53 (−1.3)	B^{AF}	−329 (−7.9)

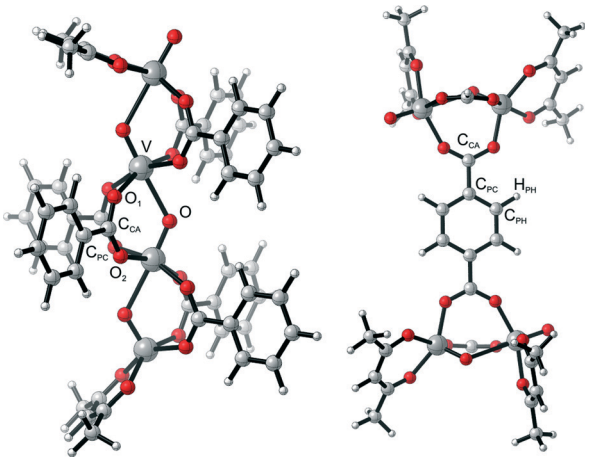

Fig. 3 Clusters on which QuickFF was applied to derive a force field for MIL-47. The atom types that are relevant for the periodic structure are indicated on the figure as well.

Table 2 Space groups for different calculated geometries obtained with PLATON

	Space group
A^{FM}	*Ima*2
A^{AF}	*Ima*2
B^{FM}	*Pnma*
B^{AF}	*Pnma*
$QuickFF_{Static}$	$Pmc2_1$
$QuickFF_{MD}$	$Pmc2_1$

building unit. Two different atom types were used for the along the inorganic chain was described by means of sixth-order polynomial function with two distinct minima, corresponding to the large and small V–O bond length. Fixed atomic charges were derived *a priori* from the molecular electron density using the Minimal Basis Iterative Stockholder scheme implemented in Horton.[41] The van der Waals interactions were added to the force field *a posteriori*. They were taken from the MM3 force field of Lii *et al.*,[42] however, a uniform scaling of 0.7 was applied to the ε-parameters and a scaling of 1.1 was applied to the σ-parameters in order to reproduce the experimental transition pressures from large pore to narrow pore and *vice versa*.[23]

All force field calculations were done with Yaff,[43] an in-house developed code for force field simulations. The non-bonded interactions were computed with a cutoff of 15 Å and the long-range electrostatics were computed using Ewald summation. Two sets of structures were generated. First we performed a regular optimization which gave a minimum on the potential energy surface. The resulting equilibrium was confirmed to be a true minimum by means of a normal mode analysis. This structure will be further referred to as QuickFF. In addition also an average structure at 300 K and 1 bar was calculated by means of a molecular dynamics run in the NPT ensemble for 800 ps with a timestep of 0.5 fs using the Nose–Hoover chain thermostat[44] and the Martyna–Tobias–Klein barostat.[45]

For practical reasons all optimizations of the crystal structure were done without constraints on the symmetry.[7] Afterwards the real symmetry of the material was verified using the PLATON software package,[46] the results are shown in Table 2.

By examining the symmetry of the calculated structures it seems that the geometries featuring the displacement are in closest agreement with the published structure from Férey *et al.* The A^{AF} and A^{FM} geometries and the structures obtained by the force field exhibit another symmetry. This analysis already points out that the displaced structures should correspond the best to the previously published geometry derived from single crystal diffraction.

An overview of all models and techniques to compare them with experimental data is shown in Fig. 4.

Results and discussion

Qualitative comparison between calculated and measured diffractograms

The simplest way to compare calculated geometries directly to the measured spectrum is a qualitative approach. The calculated geometry can be used to determine the peak positions and intensities in a diffractogram by applying simple Gaussians as a model for the diffraction peaks. Thus, an idealized diffractogram is calculated that can be compared directly with the measurements. We can see that the system with displaced vanadium chains fits the diffractogram better. In the low angle area (Fig. 5) the most important observation is the small peak at 15.5° that is only visible for the structures with displaced vanadium and corresponds with the experimental diffractogram. In the high angle region (Fig. 6) the 29.5° reflection is the main difference between the structures with and without displaced chains. This reflection is

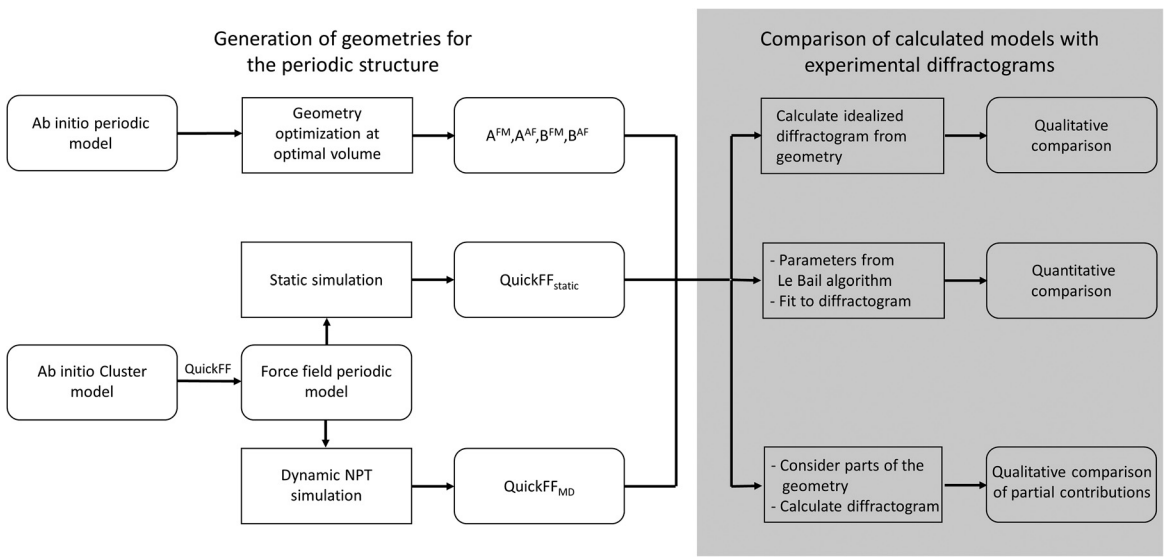

Fig. 4 Flow scheme of the applied computational procedures to compare measured and calculated diffractograms.

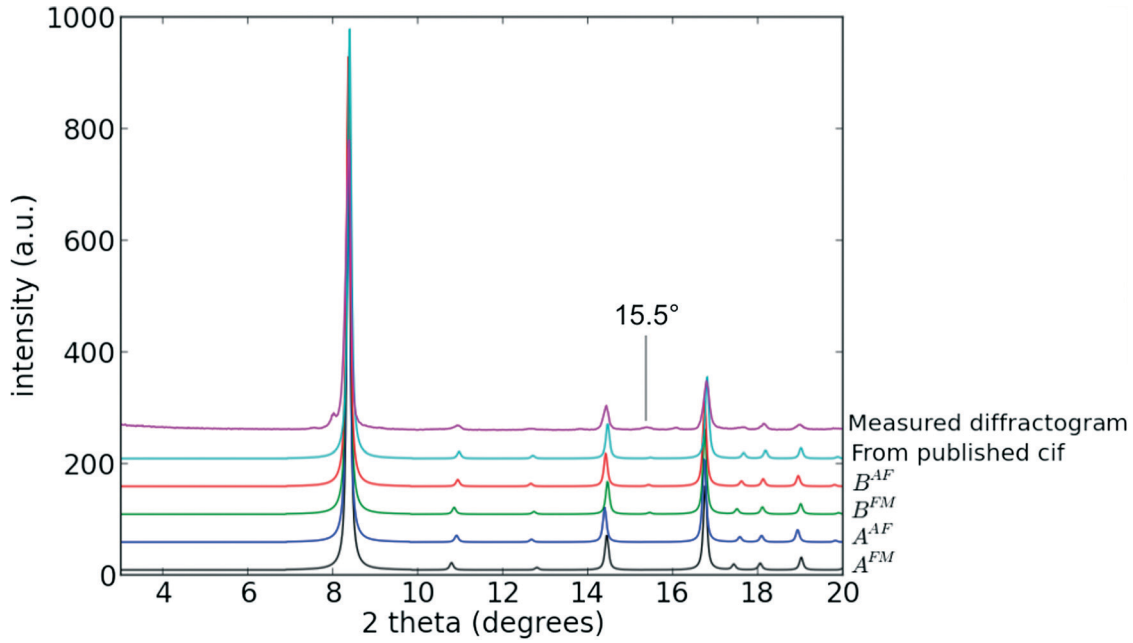

Fig. 5 Measured and calculated diffractograms at low angle (marked diffraction: (111)-plane).

also present in the measured spectrum. The same is valid for the reflection on 37.5°, but this peak is barely visible in the measured diffractogram. When only comparing the calculated diffractograms (from both DFT optimized and published geometry[22]) the geometries with displaced vanadium chains (B^{FM}, B^{AF}) appear the most favorable as they are more similar to the published one (31°, 33°, 41.5°). From an analysis of the calculated and measured diffractogram we can already conclude the importance of the displaced vanadium chains for the correct geometry, despite the fact that the energy difference in the DFT models for these two structures is small (*cf.* Table 1). However, for further analysis of the different geometries we need to verify the correspondence between a calculated geometry and a measured diffractogram quantitatively.

When comparing the geometry generated by the QuickFF force field to the measured diffractogram (Fig. 7) the differences are similar to the *ab initio* structure without the

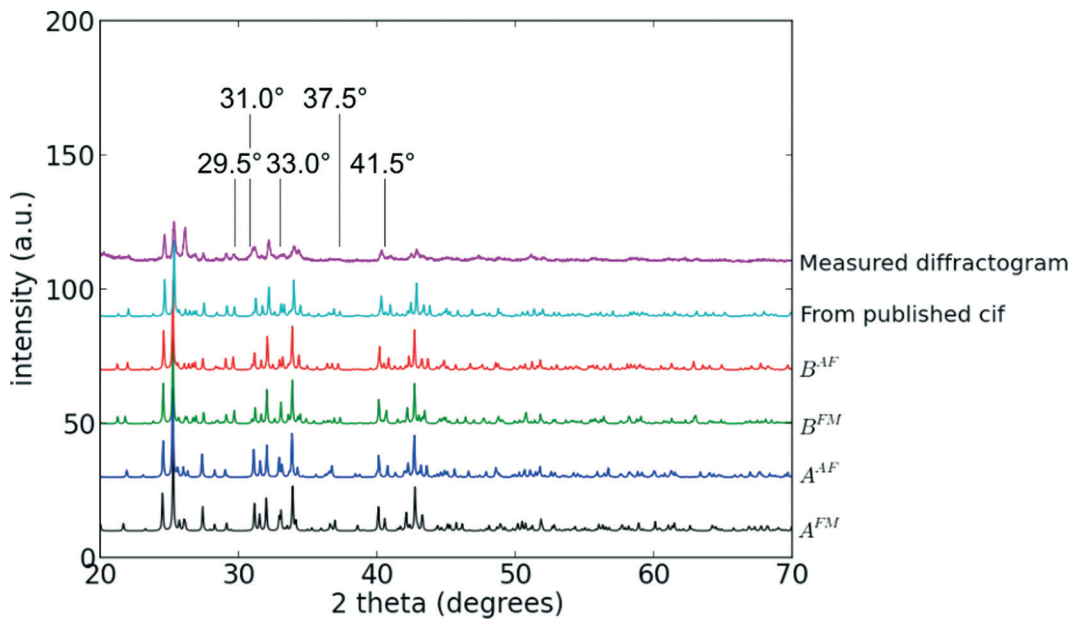

Fig. 6 Measured and calculated diffractograms at high angle. The calculated structures with displaced vanadium chains correspond well with the reported structures. The diffraction at 29.5° is the main diffraction where only the displaced structures match with the measured pattern (marked diffractions from left to right: (2,1,2)-, (2,2,2)-, (2,1,3)-, (2,1,4)-, (1,1,6)-plane).

displaced vanadium chains, both in the static geometry as in the average geometry obtained by molecular dynamics (reflections at 15.5° and 29.5°). This is what has to be expected since the training set for the force field does not include any structural parameters to induce this displacement Moreover there is a visual shift in the exact positions of the diffractions (for an overview see Fig. S1 of the ESI†) indicating that the unit cell is not well reproduced by the force field. The deviation of the unit cell by the force field most probably results from the cluster training data that were used to generate the force field. Indeed, the bond lengths in the training data obtained from B3LYP clusters are systematically longer than the bonds from the periodic calculations (Table S1 in the ESI†). This shift is significantly lower at high angles in the geometry obtained *via* molecular dynamics, showing this approach better reproduces the geometry of MIL-47(V).

Quantitative comparison between calculated geometries and measured diffractogram

One of the most important ways to analyze an XRD diffractogram is arguably the Rietveld method. Hugo Rietveld proposed an approach to fit a theoretical profile, dependent on the atomic coordinates, to a measured diffractogram using a least-squares algorithm.[47–49] With this procedure, the structure of a crystalline material can be found from powder diffraction measurements. In order to use this algorithm, a good model for the diffractogram is required. For a single, fixed phase (denoted with subscript j) this can be presented schematically as:

$$I_i^{\text{calc}} = S_{\text{F}} \sum_{k=1}^{N_{\text{peaks}}} L_k \left|F_{k,\text{j}}\right|^2 S_{\text{j}}\left(2\theta - 2\theta_{k,\text{j}}\right) P_{k,\text{j}} A_{\text{j}} + \text{bkg} \qquad (1)$$

with:

$$\left|F_{k,\text{j}}\right|^2 = m_k \left| \sum_{n=1}^{N} f_n \text{e}^{-B_n \frac{\sin^2\theta_i}{\lambda^2}} \left(\text{e}^{2\pi i\left(hx_n + ky_n + lz_n\right)}\right) \right|^2 \qquad (2)$$

This equation contains several parameters; *i.e.* a scale factor (S_{F}), peak shape (S_{j}), and the peak intensity depending of the atomic positions ($F_{k,\text{j}}$). These parameters are in turn calculated *via* an (empirical) model that contains multiple parameters, which are all fitted by the Rietveld refinement. More information on the exact form of these empirical parameters can be found in numerous textbooks on the topic.[50] However, it is important to realize what the source of these parameters is; whether they are determined by the actual structure of the chemical substance under investigation, or the experimental setup. The only parameters in eqn (1) and (2) that depend on the geometry are the peak positions (function of the unit cell parameters) and the peak intensity ($F_{k,\text{j}}$ function of the atomic positions). One can argue that other parameters, such as texture ($P_{k,\text{j}}$) are also a function of the material. However, these parameters are not calculated in the *ab initio* model, therefore they will be treated as experimental parameters that will be refined during the analysis.

This equation allows the exact calculation of the diffractogram for a given geometry (contrary to the idealized model that was presented in the previous part) provided all experimental parameters are known. Therefore a procedure is required to fit the experimental parameters *a priori*. When doing this fit, care has to be taken to avoid biases where experimental parameters are correlated to the geometry

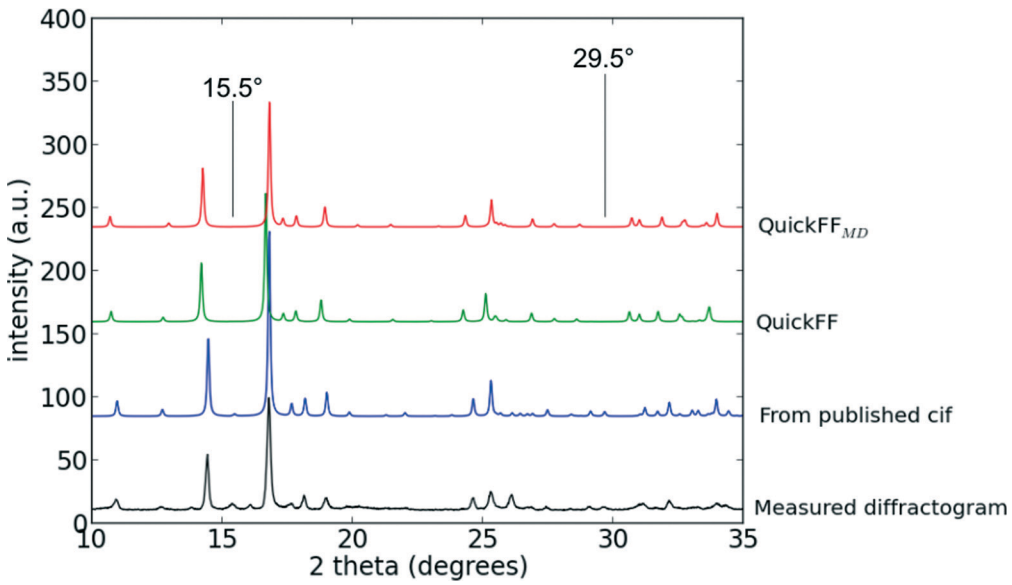

Fig. 7 Comparison between the measured diffractogram and geometries generated by the force field. QuickFF refers to the data obtained from a regular optimization while QuickFF$_{\text{MD}}$ is the structure obtained from an MD simulations at 300 K as described in the methods section. The discrepancies are due to the shifted chains not being represented in the QuickFF model (marked diffractions from left to right: (1,1,1)-, (2,1,2)-plane).

under investigation. In order to do that, a profile-only fit, in this case the Le Bail algorithm,[51,52] was employed to determine these parameters *a priori*.

The calculated diffractogram can then be compared quantitatively to the measurement after defining a measure of fit. For this we will report the Rwp value defined as (with 0% being a perfect fit):

$$\mathrm{Rwp} = \sqrt{\frac{\sum_{i=1}^{N} w_i \left(I_i^{\mathrm{exp}} - I_i^{\mathrm{calc}}\right)^2}{\sum_{i=1}^{N} w_i \left(I_i^{\mathrm{exp}}\right)^2}} \cdot 100\% \qquad (3)$$

This parameter will be assessed on different profiles. First of all it is applied on the full profile, measured for 2θ values from 3° to 70°. The second range that is considered is the so called low-angle (LA) from 3° to 20° and the third range are the high-angles (HA), going from 20° to 70°. At low angles the accuracy of the unit cell is very important. The error on the unit cell parameters will induce a shift in the diffraction positions. This will have more influence in the low angle region since this region is characterized by high but narrow peaks. In the high angle region, the geometry has a larger influence than the unit cell parameters. In this area the peak shift is larger in value, but due to the peak broadening at higher angles this shift has less influence on the fit compared to the exact geometry.

The fitting procedure is done in two steps as was discussed before: firstly a Le Bail fit is done where the unit cell parameters from the calculations are used. In this step the diffractions are modelled with a pseudo-Voight model and a three-parameter asymmetry function. On top of that, the zero shift was optimized and as a background a 10-term Legendre polynomial was used. After the profile-only fit, the atomic coordinates are introduced and the measure of fit is calculated. As a comparison, the published structure of Férey *et al.*[22] was investigated with the same algorithm. The latter structure was chosen as a literature reference since it contained the displaced vanadium chains that were shown to be crucial in the qualitative analysis.

When using the full diffractogram, the results from the first, qualitative analysis are confirmed. The structures with displaced vanadium chains provide a better fit (38.3–48.3% and 43.3–45.6%) (Table 3). Globally the B^{FM} structure seems to provide the best representation of the measured diffractogram, even better than the previously published geometry (38.3–41.45%). The difference is most clearly visible at high angles, where the atomic coordinates are the most important. At lower angles it becomes clear that the calculated unit cell parameters slightly deviate from the real structural parameters, especially for the ferromagnetic structures. This observation is not surprising since it has been reported several times that the PBE functional overestimates the unit cell parameters.[53–56] It can be concluded that the B^{FM} geometry would be the best representation of the MIL-47(V) structure, except for the unit cell parameters.

Table 3 Rwp values of the fit with a measured diffractogram with fixed unit cell during profile-only fit

	Full (3–70°)	High angle (20–70°)	Low angle (3–20°)
A^{FM}	48.27	44.25	30.26
A^{AF}	45.63	52.81	16.58
B^{FM}	38.31	39.30	21.00
B^{AF}	43.28	44.77	16.87
$\mathrm{QuickFF_{Static}}$	51.98	57.86	30.86
$\mathrm{QuickFF_{MD}}$	61.78	47.11	57.32
Published cif	41.45	45.25	16.11

For the results from the force field the agreement with the visual comparison of the diffractograms is also apparent. While the overall fits are worse than the *ab initio* geometries, the molecular mechanics method adequately represents the experimental observations. The poorer fit at low angles indicates that the unit cell is not accurately represented by the force field calculation. At high angles the fit of the geometry is comparable to the *ab initio* calculations but still worse than the best QM-geometry. The geometry found by averaging over a molecular dynamics run seems to have the best correspondence with the experimental result. This is probably due to the fact that the molecular dynamics approach naturally averages the structure. Since we show the potential energy plane of this MOF is relatively flat it is imaginable that different small variations on the geometry occur in a powder which leads to an average experimental XRD diffractogram.

Partial geometrical contributions to the diffractogram

To provide more insight in the differences between geometries, segments of the crystal structures are compared *via* their diffraction pattern. When isolating a part of a geometry, the idealized diffractogram of this structure can be calculated with the same techniques as shown in the first section. At first sight it appears easier to directly compare the coordinates of the different geometries but there is one important remark to be made. An X-ray diffractogram is actually a projection of the atomic coordinates on a (2θ–intensity)-graph, and like every projection to a lower dimension, some information is lost. By considering only parts of the structure one can deduce which geometrical features induce changes in the diffractogram. This partial diffractogram approach can give significant insight into the structure refinement. Of course, these patterns cannot be compared to an experimental diffractogram, thus as a reference the published geometry from single crystal measurements is used. In a first step only the vanadium atoms are considered, since the position of the heaviest atoms has the most influence on the diffractogram, it is a logical step to use this as a starting point. By considering parts of the model much more differences become visible and an even better distinction between various structures can be made compared to the diffractogram obtained by considering the full geometry. The conclusions from the previous

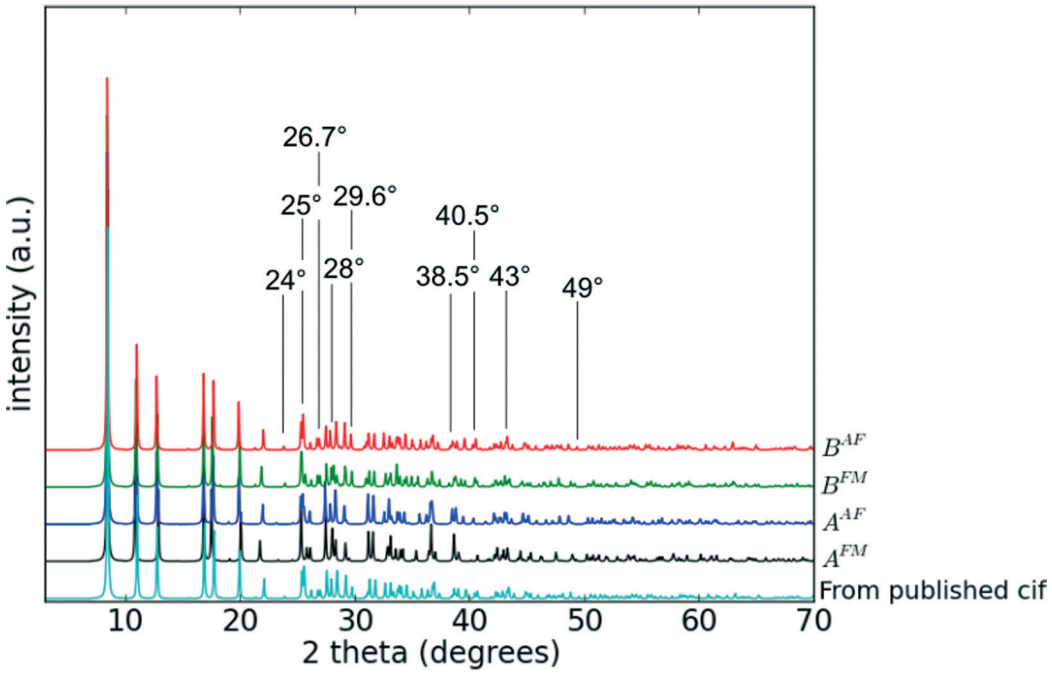

Fig. 8 Comparisons when considering only the vanadium chains.

methods are clearly confirmed here, there is a large difference between the structure with and without displaced vanadium chains (Fig. 8). The structure with displaced chains has the best agreement with the published geometry (*i.e.* the reflections at 24°, 26.7°/26.9°and 29.6°). There is also a visible difference between the FM and AF model with displaced vanadium chains. The latter variant corresponds better to the published structure (reflections at 25.5°, 28°, 38.5°, 40.5°, 43°, 49°).

The same conclusions are valid when considering only the linkers (Fig. 9) although fewer differences can be seen. Contrary to the results with the vanadium chains, the differences between the FM and AF structures are the most pronounced in the organic linkers, with the B^{AF} geometry fitting the published structure the best (reflections on 25°, 28.3°, 39.5°). The geometrical difference between the structure with and without displaced vanadium chains is very limited for the linkers and is only shown in the relatively small reflection at 15°.

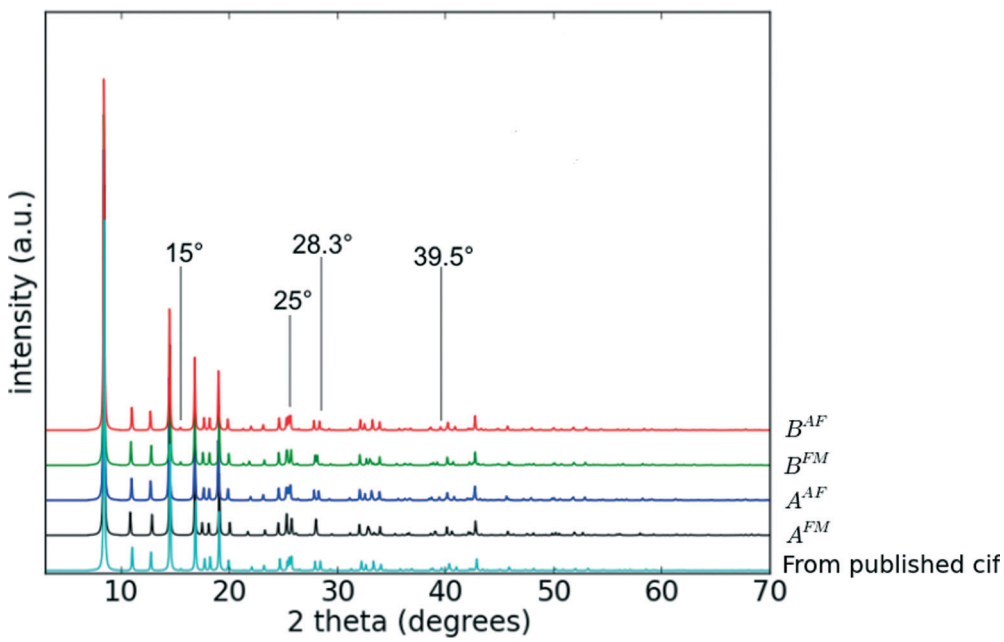

Fig. 9 Comparisons when considering only the linkers.

Generally, the linkers barely influence the calculated diffractogram, compared to the vanadium chains, even though their geometrical variations are much more pronounced, as can be seen by comparing the left and right panel of Fig. 1.

With this comparison it can be concluded that the B^{AF} structure is in close agreement with the published geometry, and the main differences between the structures are indeed a consequence of the geometry of the vanadium chains. The presented partial geometry approach allows to visualize the difference between geometries in more detail since only parts of the geometry are considered. It can again be seen that the displacement of vanadium chains is clearly visible while the different electronic structures induce only smaller geometrical differences.

The same exercise can be done for the force field geometries, as can be seen in Fig. S2 and S3 of the ESI.† The analysis shows that the main differences between the calculated and published geometries are to be found in the vanadium chains. The difference between the model derived from static calculations and the one from molecular dynamics can also be seen here, with the latter being in better agreement with the published geometry. This again shows the beneficial effect of the structure averaging by molecular dynamics calculations.

Conclusions

In this paper a methodology is presented to directly compare theoretically predicted geometries for crystalline materials to experimental X-ray diffractograms. The method has been applied on the well-studied case of the MIL-47(V) material. MOFs are particularly challenging for accurate structure determination due to their often flat potential energy surface. Herein we propose to directly compare theoretically determined diffractograms using a variety of input geometrical data with experimental X-ray diffractograms. Both a qualitative procedure where the diffractograms are compared visually and a quantitative procedure based on Rietveld's model was proposed.

As a case study the MIL-47(V) material was chosen. High-level *ab initio* calculations on this material yielded several possible geometries with comparable energies. By comparing these results to a well-resolved X-ray diffractogram the geometry with displaced vanadium chains and a ferromagnetic electronic structure, B^{FM}, was identified as being the most plausible. Especially the displacement in the vanadium chains appears to be crucial, despite the displaced geometry being energetically very close to the non-displaced variant. Next to the *ab initio* calculations, a force field for this material was constructed using a generic tool, namely the QuickFF methodology. Herein a force field is constructed from *ab initio* cluster data. In order to validate this force field the same procedures were employed. It was found that the proposed force field was able to predict the geometry of the MOF very well up to the small displacement of the vanadyl chains which was not surprising as this shift was not incorporated in the two clusters of Fig. 3, that are figuring as reference data for the force field construction. In addition, the concept of the use of the two clusters in the force-field determination also leads to a prediction of a too large unit call for MIL-47(V) due to overestimation of bond lengths by the DFT reference calculations. However, overall the generated molecular dynamics geometry of the force field yields satisfactory agreement with the X-ray diffractograms.

The decomposition of the global structure into two partial structures with a separate derivation of the X-ray diffractogram learns that the position of the vanadium chains has a significant impact on the XRD pattern while the shape of the linkers has significantly less influence. This conclusion is valid for both the *ab initio* structure as for the molecular mechanics structure. This tool allows to determine the importance of certain parts of the geometry for the powder pattern, unbiased by visual structural differences. While the B^{FM} structure provided the best correspondence to the measured X-ray diffractogram it appears that the B^{AF} geometry is in closer agreement with the structure refined from single crystal data.

Generally it can be concluded that the tools presented here to compare theoretical structures are very versatile and easy to use, the procedure that should be followed is shown in the flow scheme (Fig. 4). Powder patterns obtained by laboratory-scale diffractometers can be used to refine the fine structure of a very complex material by choosing the most well-suited geometry from *ab initio* calculations. This method is very useful when accurate geometries are necessary for applications such as adsorption, mechanical properties *etc.* Especially in the case where no single crystals are available it can prove crucial for structure resolution. Moreover, this method can assist in the design of new force field models for this crystalline materials by comparing the geometries obtained by it directly to experimental data.

Acknowledgements

The authors acknowledge financial the support from the European Research Council for funding through the European Community's Seventh Framework Programme (FP7(2007-2013) ERC Grant Agreement 240483). We are grateful to the Research Board of Ghent University and the Foundation of Scientific Research–Flanders (FWO) for support. T. B. is grateful for the support from UGent GOA grant 01G00710. L. V. is an aspirant fellow at the FWO. D. E. P. V. is a postdoctoral researcher funded by the Foundation of Scientific Research-Flanders (FWO) (project no. 12S3415N). The computational resources (Stevin Supercomputer Infrastructure) and services used in this work were provided by the VSC (Flemish Supercomputer Center), funded by Ghent University, the Hercules Foundation and the Flemish Government – department EWI.

Notes and references

1 M. Y. Sun, A. E. Nelson and J. Adjaye, *J. Phys. Chem. B*, 2006, **110**, 2310–2317.

2 P. Kuhn, M. Antonietti and A. Thomas, *Angew. Chem., Int. Ed.*, 2008, **47**, 3450–3453.
3 P. Cote, H. M. El-Kaderi, H. Furukawa, J. R. Hunt and O. M. Yaghi, *J. Am. Chem. Soc.*, 2007, **129**, 12914–12915.
4 G. Ferey, C. Mellot-Draznieks, C. Serre, F. Millange, J. Dutour, S. Surble and I. Margiolaki, *Science*, 2005, **309**, 2040–2042.
5 M. E. Schweinefuss, S. Springer, I. A. Baburin, T. Hikov, K. Huber, S. Leoni and M. Wiebcke, *Dalton Trans.*, 2014, **43**, 3528–3536.
6 D. E. P. Vanpoucke, J. W. Jaeken, S. De Baerdemacker, K. Lejaeghere and V. Van Speybroeck, *Beilstein J. Nanotechnol.*, 2014, **5**, 1738–1748.
7 D. Vanpoucke, K. Lejaeghere, M. Waroquier, V. Van Speybroeck and A. Ghysels, *J. Phys. Chem. C*, 2015.
8 S. Biswas, D. E. P. Vanpoucke, T. Verstraelen, M. Vandichel, S. Couck, K. Leus, Y.-Y. Liu, M. Waroquier, V. Van Speybroeck, J. F. M. Denayer and P. Van Der Voort, *J. Phys. Chem. C*, 2013, **117**, 22784–22796.
9 Y. G. Chung, J. Camp, M. Haranczyk, B. J. Sikora, W. Bury, V. Krungleviciute, T. Yildirim, O. K. Farha, D. S. Sholl and R. Q. Snurr, *Chem. Mater.*, 2014, **26**, 6185–6192.
10 K. V. Lawler, Z. Hulvey and P. M. Forster, *Phys. Chem. Chem. Phys.*, 2015, **17**, 18904–18907.
11 J. K. Bristow, D. Tiana and A. Walsh, *J. Chem. Theory Comput.*, 2014, **10**, 4644–4652.
12 M. A. Addicoat, N. Vankova, I. F. Akter and T. Heine, *J. Chem. Theory Comput.*, 2014, **10**, 880–891.
13 S. Bureekaew, S. Amirjalayer, M. Tafipolsky, C. Spickermann, T. K. Roy and R. Schmid, *Phys. Status Solidi B*, 2013, **250**, 1128–1141.
14 L. Vanduyfhuys, S. Vandenbrande, T. Verstraelen, R. Schmid, M. Waroquier and V. Van Speybroeck, *J. Comput. Chem.*, 2015, **36**, 1015–1027.
15 L. Vanduyfhuys, T. Verstraelen, M. Vandichel, M. Waroquier and V. Van Speybroeck, *J. Chem. Theory Comput.*, 2012, **8**, 3217–3231.
16 H. Fang, P. Kamakoti, P. I. Ravikovitch, M. Aronson, C. Paur and D. S. Sholl, *Phys. Chem. Chem. Phys.*, 2013, **15**, 12882–12894.
17 S. L. C. Moors, K. De Wispelaere, J. Van der Mynsbrugge, M. Waroquier and V. Van Speybroeck, *ACS Catal.*, 2013, **3**, 2556–2567.
18 E. Verheyen, L. Joos, K. Van Havenbergh, E. Breynaert, N. Kasian, E. Gobechiya, K. Houthoofd, C. Martineau, M. Hinterstein, F. Taulelle, V. Van Speybroeck, M. Waroquier, S. Bals, G. Van Tendeloo, C. E. A. Kirschhock and J. A. Martens, *Nat. Mater.*, 2012, **11**, 1059–1064.
19 B. K. Chang, N. C. Bristowe, P. D. Bristowe and A. K. Cheetham, *Phys. Chem. Chem. Phys.*, 2012, **14**, 7059–7064.
20 M. Vandichel, J. Hajek, F. Vermoortele, M. Waroquier, D. E. De Vos and V. Van Speybroeck, *CrystEngComm*, 2015, **17**, 395–406.
21 S. Henne, B. Bredenkotter, M. Alaghemandi, S. Bureekaew, R. Schmid and D. Volkmer, *ChemPhysChem*, 2014, **15**, 3855–3863.
22 K. Barthelet, J. Marrot, D. Riou and G. Férey, *Angew. Chem., Int. Ed.*, 2002, **41**, 281–284.
23 P. G. Yot, Q. Ma, J. Haines, Q. Yang, A. Ghoufi, T. Devic, C. Serre, V. Dmitriev, G. Ferey, C. Zhong and G. Maurin, *Chem. Sci.*, 2012, **3**, 1100–1104.
24 C. F. Macrae, I. J. Bruno, J. A. Chisholm, P. R. Edgington, P. McCabe, E. Pidcock, L. Rodriguez-Monge, R. Taylor, J. van de Streek and P. A. Wood, *J. Appl. Crystallogr.*, 2008, **41**, 466–470.
25 V. Petricek, M. Dusek and L. Palatinus, *Z. Kristallogr. - Cryst. Mater.*, 2014, **229**, 345–352.
26 S. Grimme, J. Antony, S. Ehrlich and H. Krieg, *J. Chem. Phys.*, 2010, 132.
27 S. Grimme, S. Ehrlich and L. Goerigk, *J. Comput. Chem.*, 2011, **32**, 1456–1465.
28 P. E. Blöchl, *Phys. Rev. B: Condens. Matter Mater. Phys.*, 1994, **50**, 17953–17979.
29 G. Kresse and J. Hafner, *Phys. Rev. B: Condens. Matter Mater. Phys.*, 1993, **47**, 558–561.
30 G. Kresse and J. Furthmüller, *Phys. Rev. B: Condens. Matter Mater. Phys.*, 1996, **54**, 11169–11186.
31 G. Kresse and D. Joubert, *Phys. Rev. B: Condens. Matter Mater. Phys.*, 1999, **59**, 1758–1775.
32 J. P. Perdew, K. Burke and M. Ernzerhof, *Phys. Rev. Lett.*, 1996, **77**, 3865–3868.
33 P. G. Dacosta, O. H. Nielsen and K. Kunc, *J. Phys. C: Solid State Phys.*, 1986, **19**, 3163.
34 P. Vinet, J. R. Smith, J. Ferrante and J. H. Rose, *Phys. Rev. B: Condens. Matter Mater. Phys.*, 1987, **35**, 1945–1953.
35 M. J. Frisch, G. W. Trucks, H. B. Schlegel, G. E. Scuseria, M. A. Robb, J. R. Cheeseman, G. Scalmani, V. Barone, B. Mennucci, G. A. Petersson, H. Nakatsuji, M. Caricato, X. Li, H. P. Hratchian, A. F. Izmaylov, *et al., Gaussian09*, Gaussian Inc., Wallingford CT, 2009.
36 A. D. Becke, *J. Chem. Phys.*, 1993, **98**, 5648–5652.
37 C. T. Lee, W. T. Yang and R. G. Parr, *Phys. Rev. B: Condens. Matter Mater. Phys.*, 1988, **37**, 785–789.
38 A. D. Becke, *Phys. Rev. A: At., Mol., Opt. Phys.*, 1988, **38**, 3098–3100.
39 R. Krishnan, J. S. Binkley, R. Seeger and J. A. Pople, *J. Chem. Phys.*, 1980, **72**, 650–654.
40 A. D. McLean and G. S. Chandler, *J. Chem. Phys.*, 1980, **72**, 5639–5648.
41 T. Verstraelen, K. Boguslawski, P. Tecmer, F. Heidar-Zadeh, M. Chan, T. D. Kim, Y. Zhao, S. Vandenbrande, D. Yang, C. E. González-Espinoza, P. A. Limacher, D. Berrocal, A. Malek and P. W. Ayers, *HORTON 2.0.0*, http://theochem.github.com/horton, 2015.
42 N. L. Allinger, Y. H. Yuh and J. H. Lii, *J. Am. Chem. Soc.*, 1989, **111**, 8551–8566.
43 T. Verstraelen, L. Vanduyfhuys, S. Vandenbrande and S. M. J. Rogge, *Yaff, yet another forcefield*, Available at: http://molmod.ugent.be/software/.
44 S. Nose, *Mol. Phys.*, 1984, **52**, 255–268.
45 G. J. Martyna, D. J. Tobias and M. L. Klein, *J. Chem. Phys.*, 1994, **101**, 4177–4189.
46 A. Spek, *Acta Crystallogr., Sect. D: Biol. Crystallogr.*, 2009, **65**, 148–155.
47 H. Rietveld, *J. Appl. Crystallogr.*, 1969, **2**, 65–71.

48 K. D. M. Harris and M. Tremayne, *Chem. Mater.*, 1996, **8**, 2554–2570.
49 L. B. McCusker, R. B. Von Dreele, D. E. Cox, D. Louer and P. Scardi, *J. Appl. Crystallogr.*, 1999, **32**, 36–50.
50 W. I. F. David, K. Shankland, L. B. McCusker and C. Bärlocher, *Structure Determination from Powder Diffraction Data*, OUP Oxford, 2006.
51 A. Le Bail, *Powder Diffr.*, 2005, **20**, 316–326.
52 A. Lebail, H. Duroy and J. L. Fourquet, *Mater. Res. Bull.*, 1988, **23**, 447–452.
53 E. I. Solomon, R. A. Scott and R. B. King, *Computational Inorganic and Bioinorganic Chemistry*, Wiley, 2013.
54 L. He, F. Liu, G. Hautier, M. J. T. Oliveira, M. A. L. Marques, F. D. Vila, J. J. Rehr, G. M. Rignanese and A. Zhou, *Phys. Rev. B: Condens. Matter Mater. Phys.*, 2014, **89**, 064305.
55 B. Schatschneider, S. Monaco, A. Tkatchenko and J.-J. Liang, *J. Phys. Chem. A*, 2013, **117**, 8323–8331.
56 B. B. Averkiev, Z. A. Dreger and S. Chaudhuri, *J. Phys. Chem. A*, 2014, **118**, 10002–10010.

